



Latest LHCf physics results

O. Adriani^{a,b}, E. Berti^{a,b}, L. Bonechi^a, M. Bongi^{a,b}, G. Castellini^{a,c}, R. D'Alessandro^{a,b}, M. Del Prete^{a,b}, M. Haguenaue^g, Y. Itow^{d,f}, K. Kasahara^h, K. Kawade^d, Y. Makino^d, K. Masuda^d, E. Matsubayashi^d, H. Menjo^e, G. Mitsuka^{b,d}, Y. Muraki^d, P. Papini^a, A.-L. Perrotⁱ, D. Pfeifferⁱ, S. Ricciarini^{a,c}, T. Sako^{d,f}, N. Sakurai^f, T. Suzuki^h, T. Tamura^j, A. Tiberio^{a,b}, S. Torii^h, A. Tricomi^{k,l}, W. C. Turner^m

^aINFN Section of Florence, Italy

^bUniversity of Florence, Italy

^cIFAC-CNR, Italy

^dSolar-Terrestrial Environment Laboratory, Nagoya University, Nagoya, Japan

^eGraduate school of Science, Nagoya University, Japan

^fKobayashi-Maskawa Institute for the Origin of Particles and the Universe, Nagoya University, Nagoya, Japan

^gEcole-Polytechnique, Palaiseau, France

^hRISE, Waseda University, Japan

ⁱCERN, Switzerland

^jKanagawa University, Japan

^kINFN Section of Catania, Italy

^lUniversity of Catania, Italy

^mLBNL, Berkeley, California, USA

Abstract

The LHCf experiment is dedicated to the measurement of very forward particle production in the high energy hadron-hadron collisions at LHC, with the aim of improving the cosmic-ray air shower developments models. The detector has taken data in p-p collisions at different center of mass energies, from 900 GeV up to 7 TeV, and in p-Pb collisions at $\sqrt{s} = 5.02$ TeV. The results of forward production spectra of neutrons in p-p collisions and π^0 in p-Pb collisions, compared with the models most widely used in the High Energy Cosmic Ray physics, are presented in this paper.

Keywords:

LHC, Forward physics, Hadronic interaction models

1. Brief description of the experiment

The LHCf experiment is composed by two independent detectors (Arm1 and Arm2), each made by two sampling and imaging calorimeter towers, composed of 16 tungsten layers, 16 plastic scintillator layers for energy measurement and four position sensitive layers for impact position determination. The position sensitive layers of Arm1 and Arm2 are X-Y scintillating fiber (SciFi) hodoscopes and X-Y silicon strip detectors, respectively. The transverse cross sections of calorimeter towers are 20×20 mm² and 40×40 mm² in Arm1 and 25×25 mm² and 32×32 mm² in Arm2. The detectors are

installed 140 m away from the IP1 (Atlas) LHC interaction point, inside the zero-degree neutral absorber (Target Neutral Absorber, TAN). Charged particles from the IP are swept away by the inner beam separation dipole before reaching the TAN, so that only photons mainly from π^0 decays, neutrons and neutral kaons reach the LHCf calorimeters.

The LHCf detectors are hence able to measure neutral particles in the pseudo-rapidity range from $\eta = 8.4$ to infinite (zero degree). The energy resolution of the detectors for photons and neutrons is 5% and 35%, respectively, while the position resolution in the neutral par-

ticle's reconstruction is better than $200\mu\text{m}$ for photons and a few mm for neutrons. More details of the detector performance are reported in [1, 2].

The experiment has taken data during different periods, between 2009 and 2013, both in p-p and p-Pb collisions. Here we will report on the latest analysis results, the neutron inclusive energy spectra in 7 TeV p-p collisions and the P_T vs η π^0 spectra in p-Pb collisions at $\sqrt{s} = 5.02$ TeV.

2. Neutron spectra in p-p collisions

In this section we will present some preliminary results for the inclusive neutron spectra measured by the LHCf experiment in p-p collisions at $\sqrt{s} = 7$ TeV. The data used in this analysis have been taken at the beginning of the LHC run, in 2010, in low luminosity conditions, that are optimal for the LHCf experiment.

The performance of the LHCf detectors for hadron measurements have been carefully studied by Monte Carlo (MC) simulations and confirmed by using 350 GeV proton beams at CERN-SPS. Details can be found in [3].

The analysis workflow for the neutron energy spectra measurement is similar to the workflow used for the γ analysis, described in [4]. The luminosity has been measured with the help of the LHCf front counter rates, properly normalized with the Van der Meer LHC scan. Particle identification has been carried out by looking at the longitudinal shower development, using two dimensional cuts in the L20% and L90% plane, where L20% and L90% are the longitudinal depths containing 20% and 90% of the total deposited energy, respectively. Hit position has been evaluated by using the transverse shower distribution, measured with the position sensitive layers, to optimally correct the energy measured for the leakage effects.

Due to the limited energy resolution for the neutron sample ($\approx 30\text{--}40\%$), the measured spectra should be properly unfolded to get the realistic neutron spectra. We used a multidimensional-spectra unfolding method based on Bayesian theory, relying on the two measured variables Energy and P_T .

Figure 1 shows the preliminary energy spectra of forward neutrons measured by the Arm1 detector compared with the MC predictions; the three panels correspond to the spectra measured in different regions on the small tower ($\eta > 10.76$ in the first plot) and on the large tower ($8.99 < \eta < 9.22$ in the second plot and $8.81 < \eta < 8.99$ in the third plot).

The effect of the limited energy resolution for hadrons is evident from these plots.

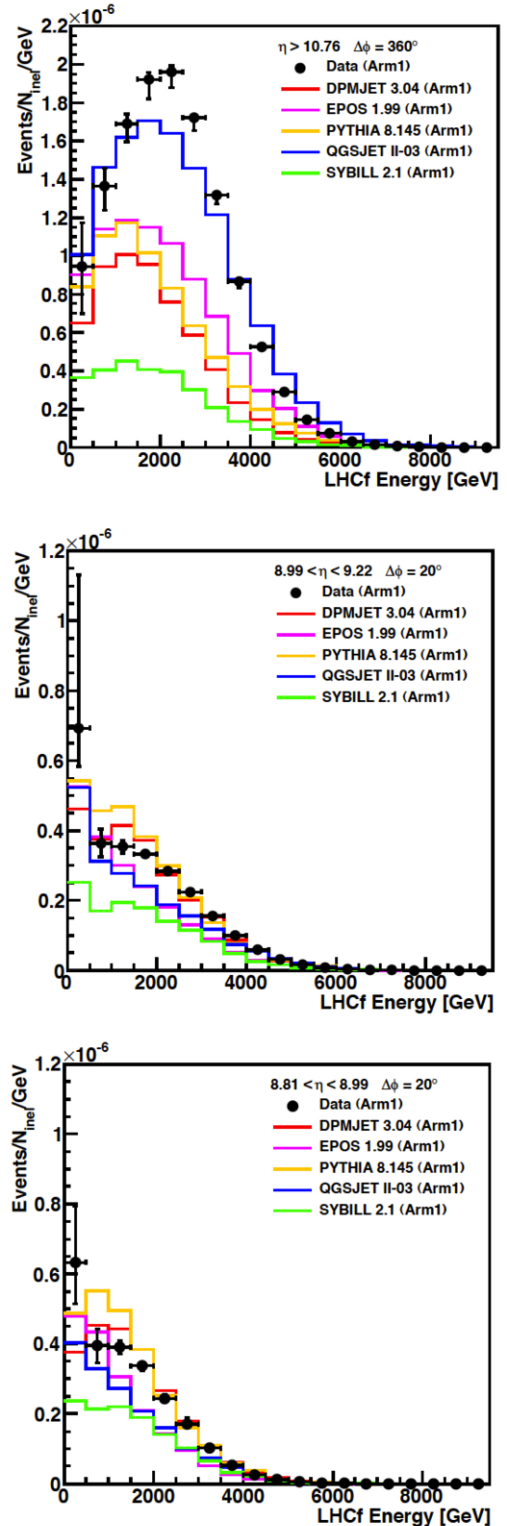


Figure 1: Preliminary neutron spectra measured by LHCf Arm1 in the $\sqrt{s} = 7$ TeV p-p collisions in three different rapidity regions.

The preliminary neutron physics spectra obtained after the unfolding procedure are presented in Figure 2. These spectra are obtained from the combination of the Arm1 and Arm2 spectra in the three above defined rapidity regions.

The most striking feature of these spectra is the pronounced high energy neutron peak in the very forward region ($\eta > 10.76$), that is predicted only by the QGSJET-II model. The presence of this peak is a clear indication of small inelasticity in the very forward p-p collision. We can hence expect that the baryons produced in the first interaction of a primary cosmic ray with the atmosphere will carry on a large fraction of the primary energy, leading to deeply penetrating VHECR induced atmospheric showers.

3. π^0 spectra in p-Pb collision at $\sqrt{s} = 5.02$ TeV

At the beginning of 2013, LHCf took data with the Arm2 detector in p-Pb collisions at the center-of-mass collision energy per nucleon of $\sqrt{s_{NN}} = 5.02$ TeV. In most of the operation time, the detector was located on the p-remnant side. The spectra measured in the proton remnant side of the high energy p-Pb collisions provide new information on the effect of the nuclear matter in the forward particle production; this kinematical region is particularly important for HECEP Physics since the interaction of the primary cosmic rays in the atmosphere occur between proton and nucleus or between nucleus and nucleus, where one of the nucleus is light component [5]. The gathered data have been analysed to extract the π^0 P_T spectra in different rapidity regions, and the measured spectra have been compared to the predictions of the various hadronic interaction models.

We present here the results that have been published in [6].

Figure 3 shows the invariant mass spectrum of the photons pairs reconstructed in the two calorimetric towers, demonstrating the excellent performances of the detector in the reconstruction of a clean π^0 sample.

Once the π^0 has been clearly identified, we can determine its transverse momentum and rapidity, allowing the measurement of the P_T vs η spectra.

We can expect that approximately half of the forward produced π^0 arise from Ultra-Peripheral collisions (UPC) of the proton in the nucleus electromagnetic field. To obtain the QCD induced spectra, the effect of the UPC should be subtracted. We have used the Weizsacher-Williams approximation to estimate the energy distribution of the virtual photons emitted by the fully ionized Pb nucleus, and we simulated the electromagnetic interactions between the virtual photons and

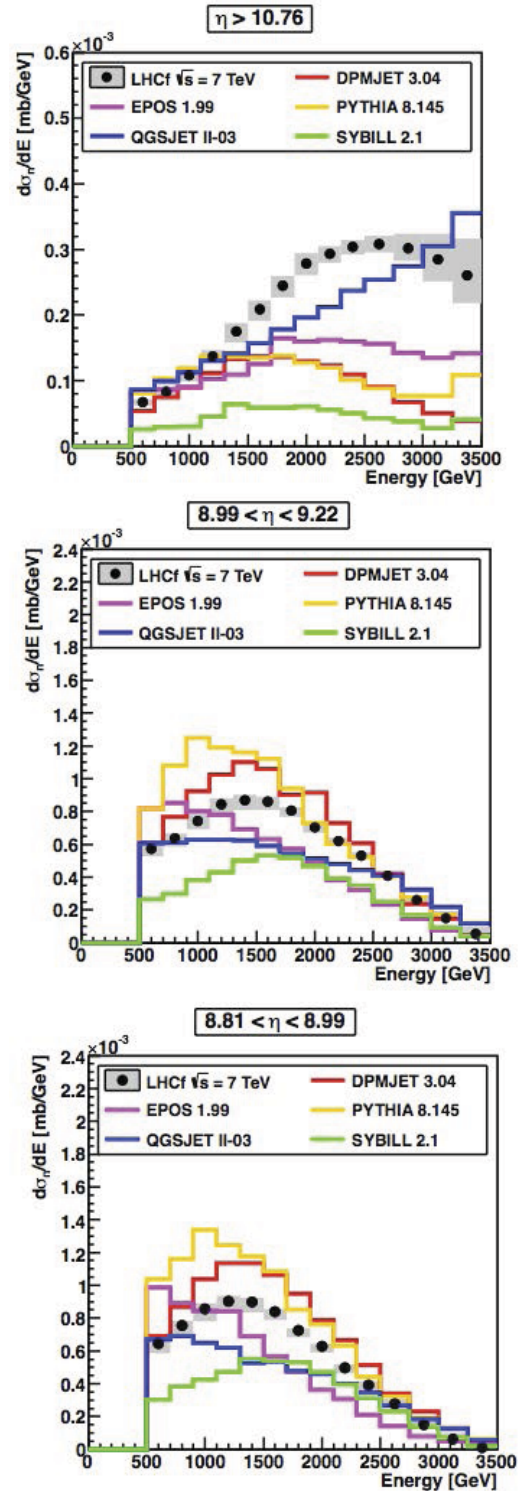


Figure 2: Preliminary unfolded neutron spectra measured by LHCf in the $\sqrt{s} = 7$ TeV p-p collisions in three different rapidity regions, compared with the models predictions.

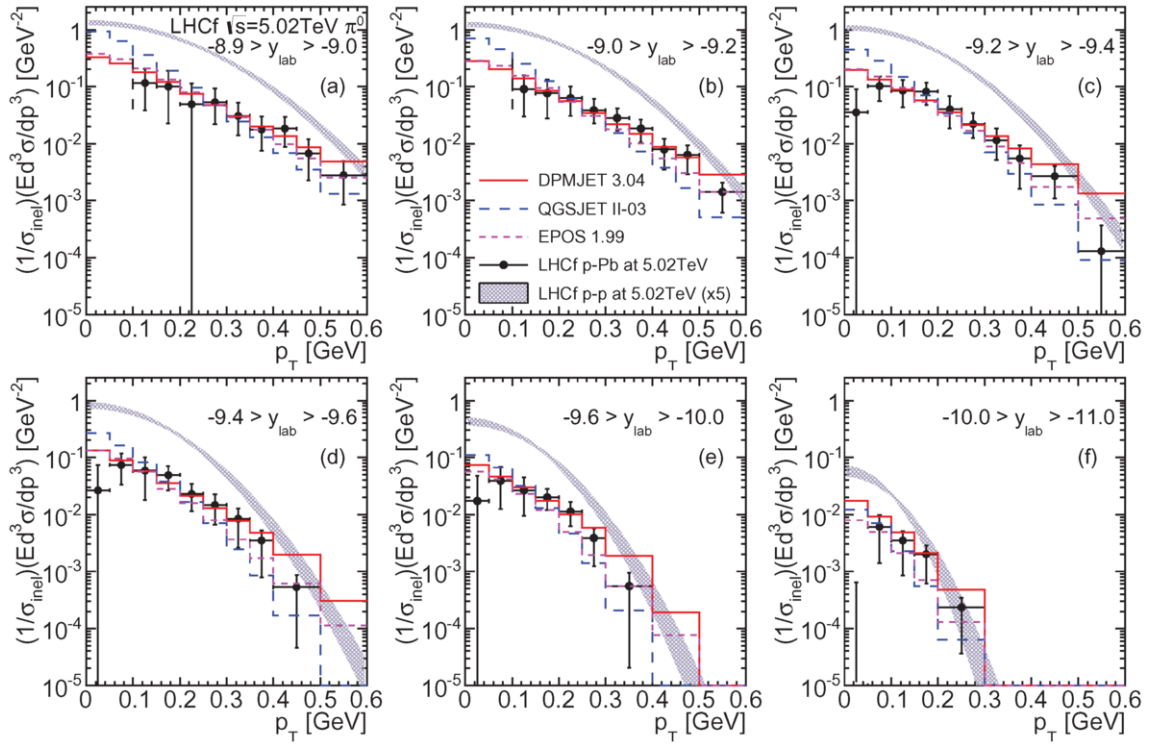


Figure 4: Experimental p_T spectra measured by LHCf in p-Pb collisions at $\sqrt{s_{NN}} = 5.02$ TeV after the subtraction of the UPC component (filled circles). Error bars indicate the total uncertainties incorporating both statistical and systematic uncertainties. Hadronic interaction models predictions and derived spectra for p-p collisions at 5.02 TeV are also shown. Figure from [6]

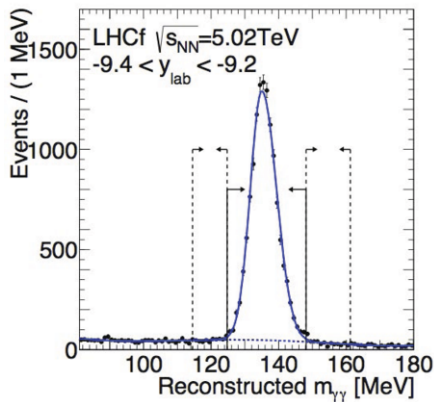


Figure 3: Invariant mass distribution of the reconstructed photon pairs in the rapidity region $-9.4 < \eta < -9.2$.

the proton with the SOPHIA model [7]. The spectra obtained in this way, after the UPC subtraction, have been compared with the spectra in p-p collisions at 5.02 TeV, obtained by interpolating the LHCf results at 2.76 TeV and 7 TeV [6] (see Figure 4). Results are also compared with the prediction of EPOS 1.99, DPMJET 3.04 and QGSJET II-03 models.

From the comparison of p-p and p-Pb results we have derived the nuclear modification factor, R_{pPb} , that is used to quantify the effect of the nuclear medium on the production of forward energetic particles. Figure 5 shows R_{pPb} measured by LHCf compared with the predictions by DPMJET 3.04, QGSJET II-03, and EPOS 1.99. The LHCf measurements, although with a large uncertainty, show a strong suppression: R_{pPb} varies from 0.1 at $p_T \approx 0.1$ GeV to 0.3 at $p_T \approx 0.6$ GeV. All hadronic interaction models predict small values of $R_{pPb} \approx 0.1$, and they show an overall good agreement with the LHCf measurements within the uncertainty.

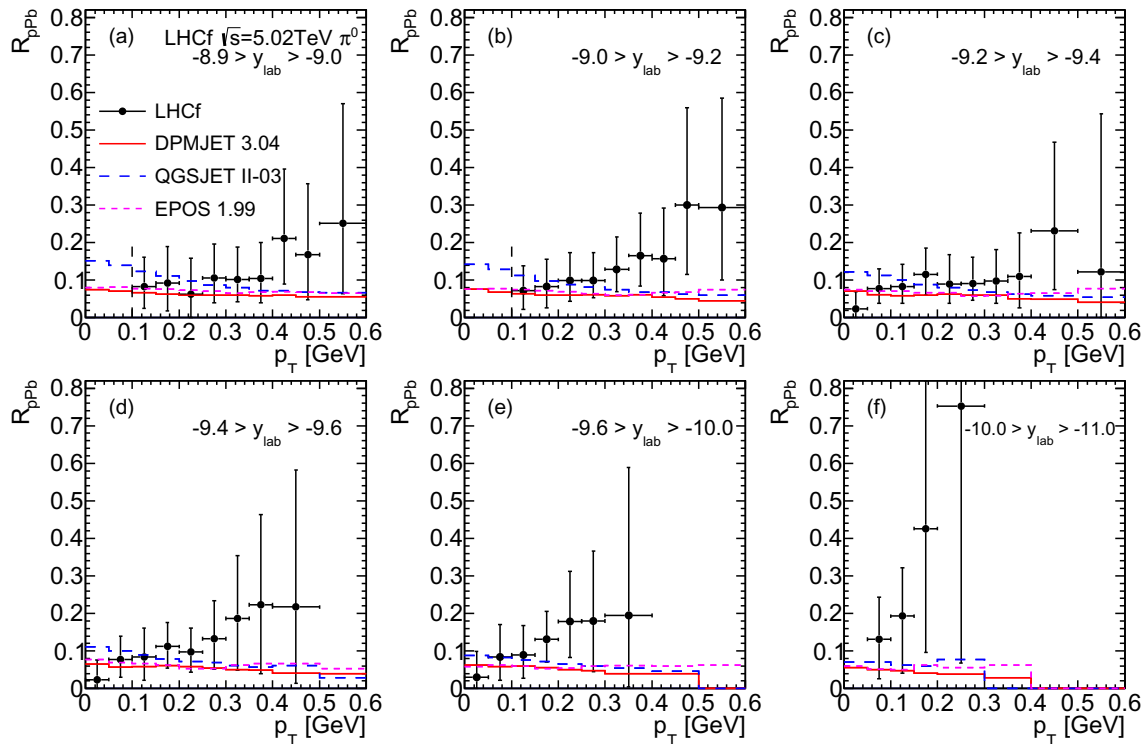


Figure 5: Nuclear modification factor for π^0 s as measured by LHCf (black solid circle) compared with the expectation of DPMJET 3.04 (red solid line), QGSJET II-03 (blue dashed line), and EPOS 1.99 (magenta dotted line). Error bars indicate the total uncertainties incorporating both statistical and systematic uncertainties. Figure from [6]

References

- [1] O. Adriani *et al.*, JINST 3 (2008) S08006.
- [2] O. Adriani *et al.*, JINST 5 (2010) P01012.
- [3] K. Kawade *et al.*, JINST 9 (2014) P03016.
- [4] O. Adriani *et al.*, PLB 703 (2011) 128.
- [5] O. Adriani, *et al.*, CERN-LHCC-2011-015. LHCC-I-021 (2011).
- [6] O. Adriani *et al.*, Phys. Rev. C 89 (2014) 065209.
- [7] A. Mucke *et al.*, Computer Physics Communications, 124 (1999) 290.